Off-center displacement of the Nb ions below and above the ferroelectric phase transition of $KTa_{0.91}Nb_{0.09}O_3$

O. Hanske-Petitpierre
Physics Department (FM-15), University of Washington, Seattle, Washington 98195

Y. Yacoby
Racah Institute of Physics, The Hebrew University of Jerusalem, Givat Ram, 91 904 Jerusalem, Israel

J. Mustre de Leon, E. A. Stern, and J. J. Rehr
Physics Department (FM-15), University of Washington, Seattle, Washington 98195
(Received 6 July 1990; revised manuscript received 7 June 1991)

We have measured the off-center displacements of the Nb ions in $KTa_{0.91}Nb_{0.09}O_3$ as a function of temperature both below and above the ferroelectric transition temperature $T_c = 85.6$ K. The purpose of these measurements was to elucidate the basic nature of the ferroelectric phase transitions in mixed perovskites. The off-center displacements were determined by x-ray-absorption fine-structure (XAFS) measurements. The data were analyzed by calculating the XAFS spectra theoretically as a function of structural and other parameters and by refining these parameters to obtain the best fit with the experimental results up to the third coordination shell. In these calculations we used curved photoelectron wave functions and took into account multiple scattering up to and including, the third-order collinear scattering. It is found that these scattering contributions are both necessary and sufficient in order to account for all the scattering contributions with a total scattering path length of 8 Å or less. At 70 K the off-center displacement, relative to the oxygen octahedra, is found to be 0.145 Å in the [111] direction. These displacements change by less than 20% from 70 K to room temperature, namely, from below to far above the phase transition. These results lead to the conclusion that the magnitude of the displacements hardly changes over a very wide temperature range. Thus, the ferroelectric transition is not displacive and the main change taking place at the phase transition is from a disordered to orientationally ordered arrangement of displacements.

I. INTRODUCTION

The fundamental nature of the ferroelectric phase transitions in oxygen perovskite materials has been the subject of a great deal of research and some controversy. One of the main questions is whether the transitions are essentially displacive or order-disorder. A great deal of experimental evidence suggests that the transitions have at least an important element of order-disorder. Most of the evidence is rather indirect showing that the symmetry of the system at the microscopic scale is broken already at the paraelectric phase far above the phase transition temperature.

The first experiments to strongly suggest the existence of some sort of disorder in the paraelectric phase were diffuse x-ray scattering measurements.[1,2] Essentially, these measurements show that there is some sort of distortion which is correlated in the [100] type directions over distances of the order of 10–50 Å. The existence of this correlation was explained in terms of the anisotropic dispersion of the transverse optic branch and its particular flatness in [100] type directions.[3] The fact that the families of diffuse scattering streaks disappear successively as the crystals transform into lower symmetry phases, led the authors to propose a very bold qualitative model for the phase transitions in these systems.[4] In essence, they proposed that, in the cubic phase, the *B*-type ions are displaced in the [111] type directions. These off-center displacements (OCD's) are correlated along [100] type directions but are otherwise random. In the lower symmetry phases, only subsets of these displacements are allowed producing a net polarization in the [100], [110], and [111] directions in the tetragonal, orthorhombic, and rhombohedral phases, respectively.

Raman experiments indicated that the local symmetry in pure crystals is broken on the microscopic scale leading to the observation of symmetry unallowed broad first-order Raman lines.[5] These effects are more difficult to observe in mixed crystals. However, using differential Raman measurements the breakdown of the local symmetry was also observed in several mixed crystals, namely $KTaO_3$:Li and $KTaO_3$:Na (Refs. 6 and 7) and later on in $KTaO_3$:Nb.[8] Weak but sharp first-order Raman lines were observed in the paraelectric phase at temperatures up to 120° K above the ferroelectric phase transition temperature. Quantitative analysis of the integrated intensity of these lines showed that it is consistent with a Halperin and Varma impurity- induced central-peak model.[7,8]

Measurements of the optical refractive index as a function of temperature also showed that the symmetry on the microscopic scale breaks down more than 100 K above the transition temperature.[9] These results show

that although the polarization vanishes above phase transition the average of the polarization squared is not zero. Thus these measurements also support the notion of disorder in the paraelectric phase. Measurements of the dynamic properties of these systems, using hyper-Raman[10,11] and ir[12] spectroscopies, were interpreted in conflicting ways. The ir results seem to show convincingly that only the last transition in $BaTiO_3$ may be triggered by a soft-mode instability. The others seem to be order-disorder transitions.

$KTa_{1-x}Nb_xO_3$ mixed crystals (KTN) which are the subject of the present study, are very interesting materials. Detailed phase diagrams of this system were measured by Perry *et al.*[13] The system undergoes three phase transitions (cubic-tetragonal-orthohombic-rhombohedral) over most of the concentration range. At low Nb concentrations, the transition temperatures come closer together, finally leading to a single cubic-rhombohedral transition. The dielectric and elastic properties of these systems for low Nb concentrations were studied in great detail.[14] The system was found to become ferroelectric at $x > 0.008$. At this concentration the transition temperature is $T_c = 0$ and the critical exponent for the temperature dependence of the dielectric constant was found to be 2 instead of the classical 1. The results were found to be consistent with the nonlinear shell model theory of Migoni *et al.*[15] over a very wide temperature range. Recently Samara[16] and Glinzuk *et al*,[17] have suggested that the system has a polar glass phase in certain temperature and concentration ranges. These results also support the existence of disorder in the macroscopically paraelectric phase.

The experimental results, discussed briefly above, suggest that many perovskite systems including KTN show some sort of disorder in the paraelectric phase, but provide no direct quantitative information on the nature, size, and temperature dependence of the OCD's involved. Electron spin resonance (ESR) experiments can provide a direct means to observe and quantitatively measure OCD's of individual ions on the microscopic scale.[18] However, the ions, which are usually important in making oxygen perovskites ferroelectric, cannot be observed in ESR. Therefore, it is necessary to find substitutional ions, that can be observed and are also similar enough to the ions they replace, in order to provide information on the system undergoing the ferroelectric transition. One such system is Mn^{4+} substituting for Ti^{4+} in $BaTiO_3$. Using this approach Müller *et al.*[19] were above to measure the OCD of Ti^{4+} in the rhombohedral phase and found it was 0.14 Å in [111] type directions. However, ESR spectra could not be observed in the higher temperature phases. In principle, X-ray-Absorption Fine-Structure (XAFS)[20] experiments, can provide direct information on the microscopic structure in the vicinity of each atom in the system. Moreover, XAFS can measure the OCD's even if they are orientationally disordered. In practice, many of the atoms, which are of interest in the oxygen perovskite crystals, are easily probed including Ta, Nb, Ti, Ba, K, Pb, and Zr. In previous work,[21] we have shown that XAFS is very sensitive to the main kinds of structural distortions that take place in the perovskites. Namely, it is sensitive to off-center displacements of the order of 0.05 Å of the *A* or *B* ions and to rotations larger than 3° of the oxygen octahedra. By using various probe atoms one can study the structure surrounding different atoms in the same system both in pure and mixed crystals. This makes XAFS an excellent tool for studying mixed crystals. XAFS provides a snapshot of the structure with an equivalent time of the order of 10^{-16} secs. Therefore, even if the distortions are dynamic in nature and the ions hop at a rate that is too fast for either magnetic resonance experiments or Raman, their displacement will be observed by XAFS. In this sense, XAFS provides complementary information to magnetic resonance methods.

Preliminary results on the OCD of Nb have been presented at conferences.[22] In this paper we present a more complete analysis and discussion of the results.

II. EXPERIMENTAL MEASUREMENTS AND RESULTS

In these experiments we used a $KTa_{0.91}Nb_{0.09}O_3$ crystal grown by Dr. D. Ritz from the Howard Hughes research laboratory using the top-seeded solution-growth method. The crystal was carefully powdered and then thinly applied on tape. In measuring the Nb edge the sample consisted of at least 8 layers of tape to produce a total absorption of 2.5 absorption lengths which guaranteed both a high degree of uniformity of the x-ray absorption across the area of the sample and negligible distortion from thickness effects. The XAFS measurements were performed on Beamline IV-1 at the Stanford Synchrotron Radiation Laboratory, using both Nb and Ta as probes. In the following we shall concentrate on the Nb probe results which were measured by fluorescence. The Ta edge results, measured by transmission, were also analyzed and are essentially similar to the results[21] in pure $KTaO_3$.

The highest phase transition temperature was directly determined by measuring the capacitance of a single crystal from the same batch as came the sample that was powdered. The single crystal was placed next to the powdered sample in a copper cell during the XAFS measurement. The cell was sealed after being filled with He gas to assure good thermal contact between the cell and the samples. Any errors in the temperature measurement would thus not affect the relative temperatures between the XAFS measurements and the phase transformations. The temperature where the capacitance was maximum was used as the value of the highest transition temperature, namely, 85.6 K. From this value and the phase diagram of Perry *et al.*[13] we determined the rhombohedral-orthorhombic-tetragonal transition temperatures as 71 and 80 K, respectively. The measurements were carried out at several temperatures, namely, 70, 78, 90, 130, 200, and 300 K. These temperatures were chosen to be below, close to and above the various ferroelectric phase transitions.

An example of the raw XAFS data, using the *K* absorption edge of Nb, is shown in Fig. 1. In this spectrum, the background has already been removed. In spite of

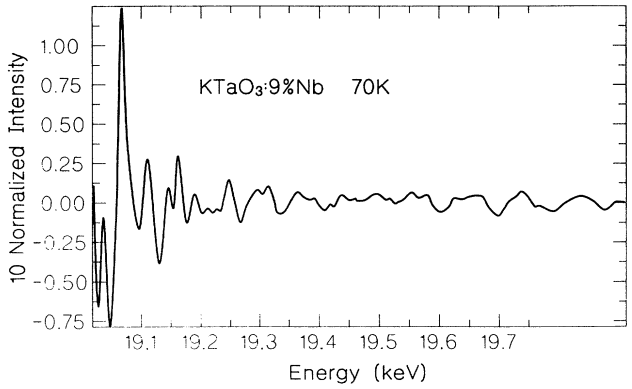

FIG. 1. Raw XAFS spectrum of $KTaO_3$:9% Nb at 70° K.

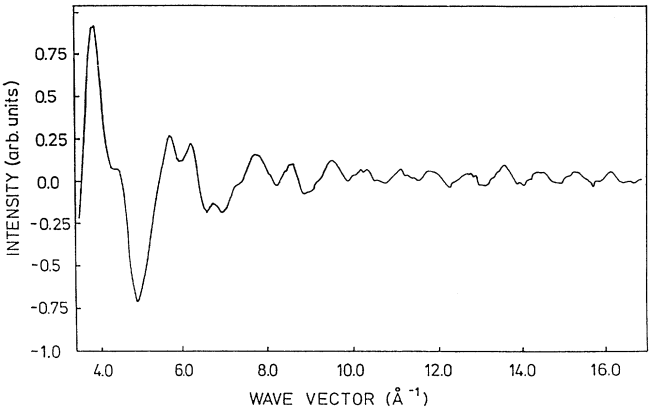

FIG. 3. The XAFS spectrum of $KTaO_3$ as a function of the photoelectron wave number.

the fact that the sample contains only 9% Nb, the signal-to-noise ratio is very good. The spectra at various temperatures are shown in Fig. 2 as a function of the photoelectron wave-number k. Notice that the $KTa_{0.91}Nb_{0.09}O_3$ spectra change only little with temperature in spite of the fact that the crystal goes through various phase transition points. Comparing these spectra to the corresponding spectrum of $KTaO_3$, shown in Fig. 3, one notices an interesting difference: Both spectra show a relatively large oscillatory structure above $k=8$ Å^{-1}, which is mainly due to scattering from the Ta neighbors. However while the amplitude of oscillations in the pure $KTaO_3$ changes only slightly with increasing wave number the spectra of $KTa_{0.91}Nb_{0.09}O_3$ show a clear beat at $k\sim 11.5^{-1}$ Å. This result indicates that the Ta-Ta distances in $KTaO_3$ are about equal to each other whereas the distances between the Nb probe and the Ta neighbors are not all equal to each other.

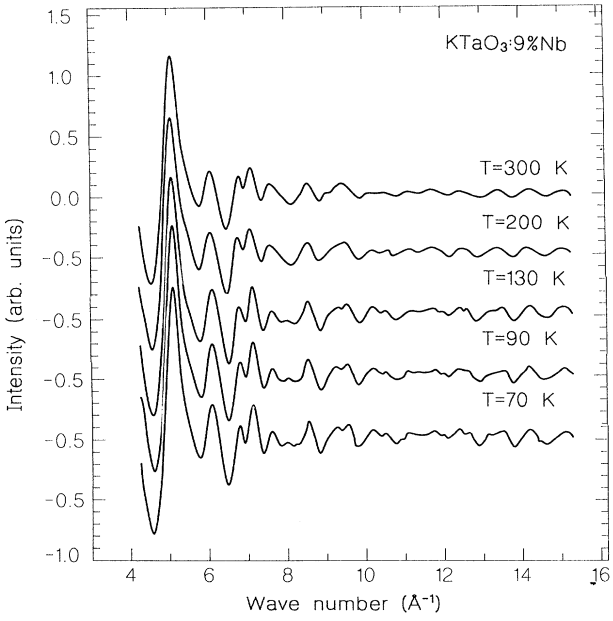

FIG. 2. The XAFS spectra of $KTaO_3$:9% Nb as a function of the photoelectron wave number, at various temperatures.

III. DATA ANALYSIS

The data analysis method has been discussed in detail by Mustre de Leon *et al.*[23,22] It is based on the refinement of a theoretical XAFS calculation to obtain the best fit with the experimental results. This analysis method has been shown to work well in several oxygen perovskite crystals including $KTaO_3$ and $NaTaO_3$.[21] Thus, the data analysis method will not be described here in full. We present here only the details relevant to the present material and the reader is referred to our previous work for a more complete discussion.

The XAFS spectra were calculated for a probe atom surrounded by the first three shells, namely, the oxygen, potassium, and tantalum shells. Altogether 21 atoms were taken into account. The first step was to calculate the muffin-tin potential using the atomic code of Descleaux.[24] As a starting point we took a self-consistent solution of the Dirac equation for each of the ions of interest. In the case of the absorbing atom we included a hole in the core state. The exchange correlation potential in this atomic calculation was approximated by the X_α potential. The α and the muffin-tin radii R were taken from tables[25] and were not allowed to vary in the refinement process. Their values are $\alpha_{Nb}=0.7039$, $\alpha_K=0.7212$, $\alpha_{Ta}=0.6932$ and $R_{Nb}=0.7$, $R_K=1.33$, $R_{Ta}=0.73$ Å. Using the muffin-tin potentials we calculated the partial scattering phase shifts which were then used in order to calculate the XAFS spectra of the different scattering configurations.

The calculation of the oxygen ion had to be done in a somewhat different way because the Descleaux[24] program does not handle negatively ionized atoms. Thus, as in the case of the other perovskites,[21] we calculated the muffin-tin potential for O^{4+} and added to it the potential contributed by six $2P$ electrons. The wave functions of these

electrons were calculated using a simple hydrogen-type model which seems to work well enough. The parameters used in this calculation were $\alpha_O=0.7445$ and $R_O=1.4$ Å.

To carry out the next step we identified all the scattering configurations involving the atoms of the first three shells up to and including triple collinear scattering. In doing so we started from the idealized cubic structure. This leads to only ten different types of scattering configurations. The single scattering contributions were calculated exactly within the single electron curved wave theory using the formulation of Rehr *et al.*[26] The double-scattering contributions were also calculated exactly using the formulation of Gurman *et al.*[27] The triple-scattering calculation was not done exactly, because it would be too time consuming. We therefore calculated it using the approximation due to Rehr *et al.*,[26] which is accurate for collinear triple scattering. At bond angles of up to 20°, the error is less than 10% in the amplitude and 0.15 radians in the phase shift.

These calculations yielded the amplitude $F_n(k)$ and the phase $\Theta_n(k)$ functions, which were needed in order to calculate the XAFS spectrum. As mentioned before, it is expected that the system is structurally distorted with respect to the idealized cubic structure we started with. To facilitate the calculation of the XAFS spectra in this case, we calculated the derivatives of the amplitude and phase functions of each configuration with respect to its structural parameters, namely, the interatomic distances and the bond angle. In the collinear scattering configurations, the first derivative with respect to the bond angle is zero. Therefore, we calculated and used the second derivative. The error introduced by this approximation was calculated and found negligible for the small distortions present in this case.[23] With this information the XAFS spectrum of any structure that does not deviate too much from the original cubic structure we started with, can be quickly calculated.

The fitting of theory and experiment was performed in the following way. The experimental data as a function of energy were fed into the fitting routine after removing the background. Using a threshold energy E_0, the data were converted into k space. E_0 can be varied within the fitting routine and refined if necessary. The data were then multiplied by k^ν, to improve the separation among the shells and by $\sin[\pi(k-k_1)/k_2-k_1)]$, to reduce the ringing in the Fourier transformed function $[k_1=k_{\min}-0.1(k_{\max}-k_{\min})$ and $k_2=k_{\max}+0.1(k_{\max}-k_{\min})]$. The theoretical data were treated in the same way. In this case we used $\nu=1.5$ to avoid overemphasizing the high energy region, where the signal-to-noise ratio is smaller. This number is smaller than the usual exponent, between 2 and 3, used in the ordinary type analysis, because here the separation among the shells is not critical.

The theoretical XAFS spectra were calculated within the fitting routine according to the following formula:

$$\chi(k)=\sum_n \mathrm{Im}\ F_n(k)\exp[i(kL_n+\Theta_n(k)+\theta+C_n/k)]\exp(-2k^2\sigma_n^2)\exp(-L_n/\lambda_n)\ . \tag{1}$$

Here, σ_n^2 and λ_n are the mean-squared displacement (MSD) and the mean free path appropriate for the n configuration, respectively. In principle their values may be different for the various configurations. However, the data do not contain enough information to determine all of them independently. The parameters that we used are therefore: σ_1^2 for the first shell single scattering, σ_2^2 for configurations involving the second shell, and σ_3^2 for configurations involving the third shell. We found, in this case, that one mean free path was sufficient for all configurations. The constant phase parameter θ and the k dependent phase corrections, C/k (where C is a constant), were introduced to correct for deficiencies in the theory as explained by Mustre de Leon *et al.*[23] As in $KTaO_3$ and $NaTaO_3$,[21] three C coefficients were used, one for each type of scattering atom. Thus, in this analysis we used the same type of variable parameters that were used successfully in analyzing the XAFS data of copper, $KTaO_3$ and $NaTaO_3$, except that in this case $\lambda_1\simeq\lambda_2$.

The structural distortion we wanted to test in this case was the OCD of the Nb ions in the [111] type directions. Since it is possible that the structure surrounding the Nb may be distorted as well we introduced three structural distortion parameters, one for each of the first three neighboring shells: d_O, d_K and d_{Ta}. The fitting between

TABLE I. The off-center displacements (d) and the mean-squared displacements (σ^2) of the first three shells relative to the Nb probe; d is in the (111) direction for all shells, while σ^2 is the component along the direction between the Nb probe and the atoms of interest.

T (K)	d_O (Å)	$10^3\sigma_O^2$ (Å^2)	d_K (Å)	$10^3\sigma_K^2$ (Å^2)	d_{Ta} (Å)	$10^3\sigma_{Ta}^2$ (Å^2)
70	0.143	2.4	0.166	0.4	0.118	0.8
90	0.152	1.6	0.165	0.6	0.118	0.5
130	0.145	2.1	0.163	1.3	0.118	0.8
200	0.135	2.5	0.181	1.4	0.121	2.6
300	0.126	3.3	0.190	1.0	0.121	2.9

theory and experiment was performed in r space. The range of data was limited in both k and r spaces. $k_{\min}$ was set to 4.0^{-1} Å because the theory is not reliable enough below this limit. $k_{\max}=16.0^{-1}$ Å is set by the end of the experimental data. The low limit of r was chosen to be 0.9 Å. Below this value, the results are sensitive to how the background subtraction is taken. The upper limit was taken to be 4 Å. In this case the highest order of multiple scattering which one needs to consider is collinear triple scattering. Under these circumstances, the total number of experimentally independent points[28] is $(2\pi)k_{\text{range}}r_{\text{range}}=25$. This number is much larger than the total number of parameters ($N_p=12$) used to fit the data.

We first fitted the 70 K data allowing all the parameters to change. In the subsequent fits only the parameters which were expected to change with temperature were allowed to change, namely, the MSD's, σ^2, and the OCD's, d. The values of the other temperature independent parameters were

$$\theta=-0.23,\quad C_{\text{O}}=1.4\ \text{Å}^{-1},\quad C_{\text{K}}=-1.6\ \text{Å}^{-1},$$
$$C_{\text{Ta}}=48\ \text{Å}^{-1},\quad \lambda_1=14\ \text{Å},\quad \lambda_2>30\ \text{Å}\ .$$

The mean-squared displacements (MSD's) and the OCD's are presented for the different temperatures in Table I.

IV. DISCUSSION

The real and imaginary parts of the Fourier transforms of the experiments and theoretical spectra can be seen in Fig. 4. The absolute values are shown in Fig. 5. As can be seen, the quality of the fit is good for all temperatures in the fitting range between 0.9 and 4.0 Å. In Fig. 6 we present the Fourier transforms of the contributions of the first three shells, namely, single scattering from the first and second shells and the sum of the single, collinear double, and collinear triple scattering from the third shell. In addition, we show the noncollinear scattering contribution from the Nb-O-K-Nb configuration. Notice, that this contribution is not small by any means. As in the case of $KTaO_3$ and $NaTaO_3$ (Ref. 21) the collinear double and triple scattering contributions turn out to be larger than the single scattering contribution from the third shell. Moreover, it is clear, that the contributions of the second and third shells cannot be reliably separated from each other. Thus, the more sophisticated analysis carried out here is indeed needed to obtain the information contained in the experimental data.

The results in Table I show that the displacement of the O, K, and Ta shells relative to the Nb probe are about equal. This means that approximately the Nb ion is displaced relative to these shells by 0.145 Å. The displacement of the Nb relative to the Ta and oxygen shells can be directly observed in the data. The beat at $\sim 11.5^{-1}$ Å is due to the Nb displacement relative to the Ta neighbors. The splitting in the first oxygen shell seen in Fig. 5 is due to the displacement of the oxygen shell relative to the Nb. In contrast, the oxygen shell of $KTaO_3$ shown for comparison in Fig. 7, has indeed the form of a well-behaved unsplit shell.

The values of the OCD of the Nb relative to the oxygen and Ta shell are accurate to within 0.01 Å. Thus, the difference between d_{O} and d_{Ta} is experimentally significant. It means that the Ta shell is also displaced at

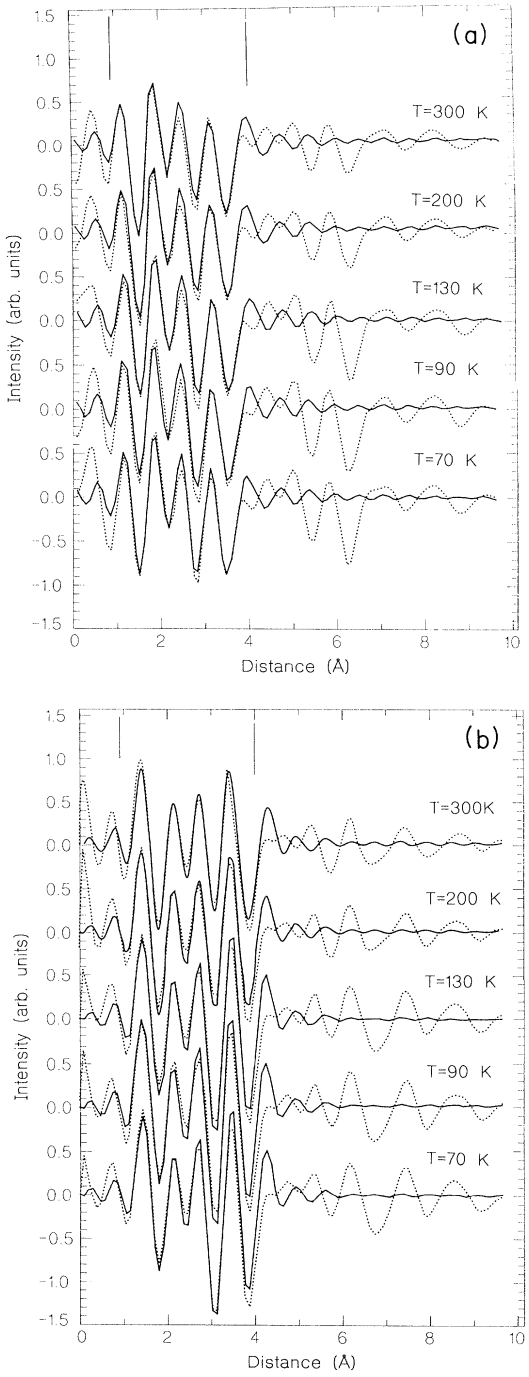

FIG. 4. Comparison between the Fourier transforms of the experimental (dotted line) and theoretical (solid line) XAFS spectra for various temperatures. (a)—Real part; (b)—imaginary part. Notice that the fit between theory and experiment was performed between 0.9 and 4 Å as marked by the two vertical lines on top.

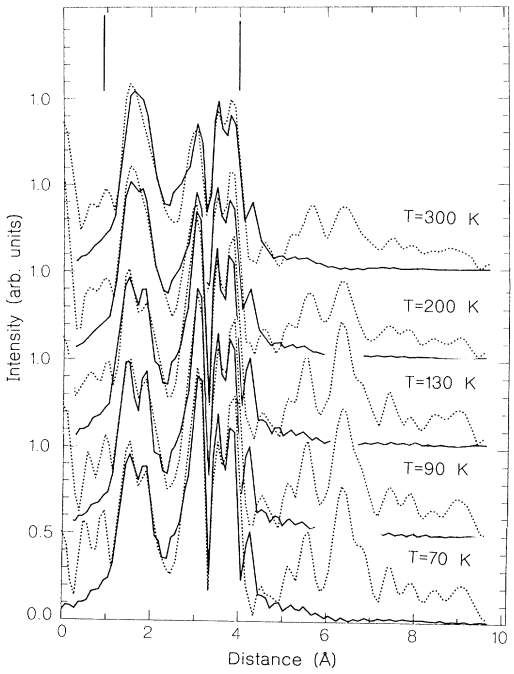

FIG. 5. Comparison between the absolute values of the Fourier transforms of the experimental (dotted line) and theoretical (solid line) XAFS spectra for various temperatures. Notice that the fit between theory and experiment was performed between 0.9 and 4 Å as marked by the two vertical lines on top.

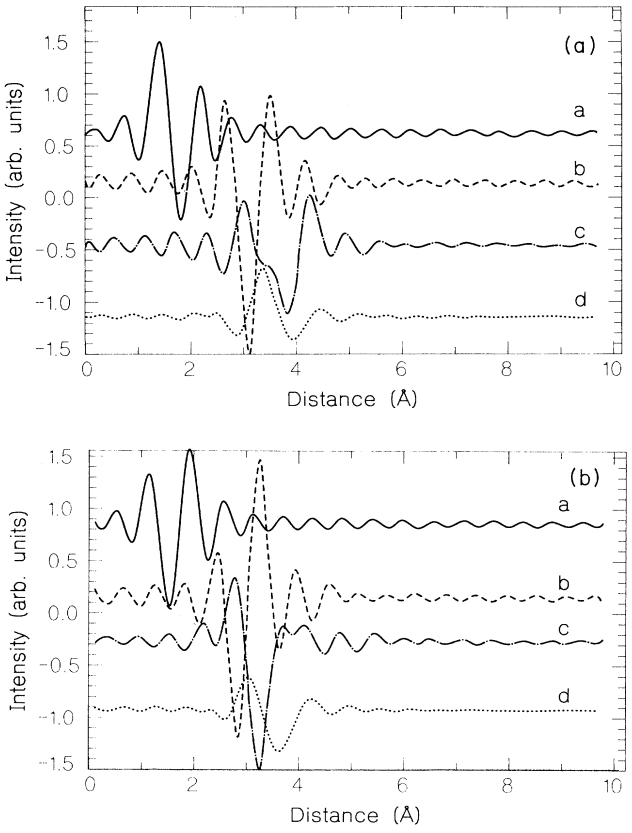

FIG. 6. Various theoretical contributions to the Fourier transform of the XAFS spectrum of $KTaO_3$:9% Nb. The real parts are shown in (a), the imaginary parts in (b). a—single scattering from the oxygen shell; b—single scattering from the potassium shell; c—single, collinear double, and collinear triple scattering from the Ta shell; d—noncollinear scattering contribution of the Nb-O-K-Nb configurations.

low temperatures relative to the oxygen shell but only by about 0.025 Å. This displacement goes to zero at 200 K and higher. The results for the K shell, especially at higher temperatures, were found to be less reliable. Thus, the difference between the K and O OCD's, observed at higher temperatures, are probably within the uncertainty of these results.

The fact, that the OCD's are much larger than the square root of the MSD's, means that the OCD is not merely an effect of anharmonicity. This is consistent with the Raman results which show that the symmetry is broken on time scales longer than 10^{-10} sec.[8] The MSD, σ^2_O, between the Nb and the oxygens is equal within the experimental error to that in pure $KTaO_3$ at room temperature.[21] The same is true for σ^2_K. On the other hand, σ^2_{Ta} at room temperatures is larger than that in $KTaO_3$ at the same temperature. This means that the Ta-Ta motions in $KTaO_3$ are much better correlated with each other, than the Nb-Ta at the same temperature.

Comparison of the temperature dependence of the OCD's measured by XAFS and the temperature dependence of the integrated intensity of the first-order Raman lines shows an interesting difference. While the OCD's hardly change all the way to room temperature, the integrated Raman line intensity decreases and practically disappears at about 120 K above the transition. The

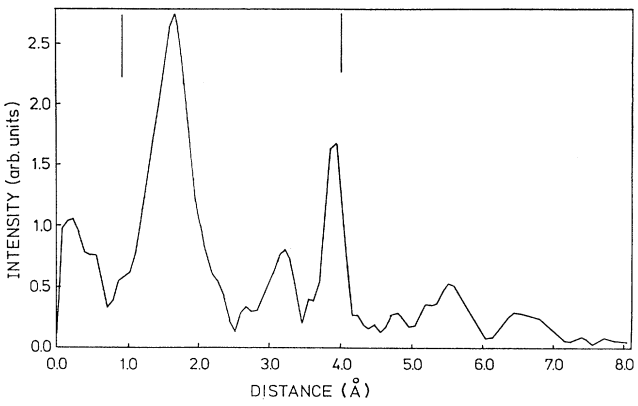

FIG. 7. The absolute value of the Fourier transform of the XAFS spectrum of $KTaO_3$ at room temperature.

reason for this difference is that the Nb off-center displacements are dynamic. At low temperatures the hopping rate among equivalent positions is slow compared to Raman measuring time of about 10^{-10} sec. As the temperature increases the hopping rate becomes too high ($\gg 10^{10}\text{sec}^{-1}$) leading to the disappearance of the first-order Raman lines.

The fact that Nb is displaced off-center at temperatures far above the phase transition temperature suggests that this OCD is not a cooperative effect. Further evidence for this is the independence of the value of the OCD on Nb concentration. Measurements[21,29–31] from a few percent Nb to 100% Nb show the same value of the OCD within experimental uncertainties of 10%. This suggests that the off-center displacement is dominated by the short-range interaction between the Nb and its near neighbors and does not depend significantly on Nb-Nb interaction.

The weak dependence, if any, of the magnitude of the OCD on temperature and concentration indicates that, at the ferroelectronic transition, the $KTaO_3$:Nb system changes from an orientationally disordered to an orientationally ordered state.

V. SUMMARY

The results presented here show that the more sophisticated analysis which was used here is essential to understand and more fully use the information contained in the XAFS spectra. We have shown that collinear double and triple scattering contributions are large relative to the corresponding single scattering contribution and even the noncollinear Nb-O-K-Nb contribution cannot be neglected. Furthermore, the second band of the absolute value of the Fourier transform contains three peaks, yet it is due to the contributions of two shells only. The deep minimum between the first and the second peaks is an antiresonance and not the boundary between second- and third-shell contributions. This result emphasizes that caution should be used in identifying peaks beyond the first in the magnitude of the Fourier transform as actual shells of atoms.

The experimental results and the analysis show that the Nb ions are indeed displaced off center already at temperatures far above the phase transition temperature. The magnitude of these displacements varies by less than 20% from a temperature which is about 20 K below to 200 K above the highest phase transition temperature. The magnitude of the square root of the MSD about the off-center position is much smaller than the OCD itself. These results added to the independence of the magnitude of the OCD on concentration indicate that the OCD is a property of the individual Nb ion and the nature of its interaction with its near neighbors, and the ferroelectric transition in $KTaO_3$:Nb is not displacive and involves an orientational order-disorder transition of the Nb ion displacements.

ACKNOWLEDGMENTS

The research reported here was supported by U. S.-Israel Binational Science Foundation under Contract No. 84-00257 and the U.S. Department of Energy under Contract Nos. DE-A505-80- ER10742 and DE-FG06-84ER45163.

[1]R. Comes, M. Lambert, and A. Guinier, Acta Crystallogr. **A26**, 244 (1970).
[2]R. Comes, R. Currat, F. Denoyer, M. Lambert, and A. Quittet, Ferroelectrics **12**, 3 (1976).
[3]R. Comes and G. Shirance, Phys. Rev. B **5**, 1886 (1972).
[4]R. Comes, M. Lambert, and A. Guinier, Solid State Commun. **6**, 715 (1968).
[5]A. M. Guittet and M. Lambert, Solid State Commun. **12**, 1053 (1973).
[6]Y. Yacoby and S. Just, Solid State Commun. **15**, 715 (1974).
[7]Y. Yacoby, Z. Phys. B **41**, 269 (1981).
[8]Y. Yacoby, Z. Phys. B **31**, 275 (1978).
[9]G. Burns and F. H. Dacol, Ferroelectrics **37**, 661 (1981).
[10]H. Vogt, J. A. Sanjurjo, and G. Rossbroich, Phys. Rev. B **26**, 5904 (1982).
[11]H. Vogt, Phys. Rev. B **36**, 5001 (1987).
[12]F. Gervais, Ferroelectrics **53**, 91 (1984).
[13]C. H. Perry, R. R. Hayes, and N. E. Torenberg (unpublished).
[14]D. Rytz, U. T. Höchli, and H. Bilz, Phys. Rev. B **22**, 359 (1980).
[15]R. Migoni, H. Bilz, and D. Bauerle, Phys. Rev. Lett. **37**, 1155 (1976).
[16]G. A. Samara, in Proceedings of the 6th International Meeting on Ferroelectricity [Jpn. J. Appl. Phys. **24**, Suppl. 80 (1985)].
[17]M. D. Glinzuck, A. A. Karmazin, and I. M. Smolyaninov, Ukr. Fiz. Zh. **33**, 110 (1988).
[18]K. A. Müller, in *Nonlinearity in Condensed Matter,* edited by A. R. Bishop (Springer Verlag, Heidelberg, 1986), p. 234.
[19]K. A. Müller, W. Berlinger, K. W. Blazey, and J. Albers, Solid State Commun **61**, 21 (1987).
[20]E. A. Stern and S. M. Heald, in *Handbook on Synchrotron Radiation,* edited by E. E. Koch (North-Holland, Amsterdam, 1983), Vol. 1, Chap. 10.
[21]Y. Yacoby, J. Mustre de Leon, E. A. Stern, J. J. Rehr, and B. Rechav (unpublished).
[22]O. Hanske-Petitpierre, E. A. Stern, and Y. Yacoby, J. Phys. C8 **47**, 675 (1986); J. Mustre de Leon, Y. Yacoby, E. A. Stern, J. J. Rehr, and M. Dell'ariccia, Physica B **158**, 263 (1989).
[23]Y. Yacoby, J. Mustre de Leon, E. A. Stern, and J. J. Rehr, Phys. Rev. B **42**, 10 843 (1990).
[24]J. Desscleaux, J. Phys. B **4**, 631 (1971); Comput. Phys. Commun. **9**, 31 (1975).
[25]K. Schwarz, Phys. Rev. B **5**, 2466 (1972); Theor. Chem. Acta **34**, 225 (1974).
[26]J. J. Rehr, R. C. Albers, C. R. Natoli, and E. A. Stern, Phys.

Rev. B **34**, 4350 (1986).
[27]S. J. Gurman, N. Binsted, and I. Ross, J. Phys. C **17**, 143 (1984).
[28]P. A. Lee, P. H. Citrin, P. Eisenberger, and B. M. Kincaid, Rev. Mod. Phys. **53**, 769 (1981).
[29]O. Pettipierre, Ph.D. thesis, University of Washington (1986).
[30]A. W. Hewat, J. Phys. C **6**, 2559 (1973).
[31]K. H. Kim, W. T. Elam, E. F. Skelton, J. P. Kirkland, and R. A. Neiser, Phys. Rev. B **42**, 10 724 (1990).